



## Supporting Information

for *Macromol. Rapid Commun.*, DOI: 10.1002/marc.201500208

Characterization of Diblock Copolymer Order–Order  
Transitions in Semidilute Aqueous Solution Using  
Fluorescence Correlation Spectroscopy

Christopher G. Clarkson, Joseph R. Lovett, Jeppe Madsen,  
Steven P. Armes,\* Mark Geoghegan\*

**Supporting Information for:**

**Characterization of Diblock Copolymer Order-Order  
Transitions in Semi-Dilute Aqueous Solution using  
Fluorescence Correlation Spectroscopy**

C. G. Clarkson,<sup>a</sup> J. R. Lovett,<sup>b</sup> J. Madsen,<sup>b</sup> S. P. Armes,<sup>b</sup> and M. Geoghegan<sup>a</sup>

## Experimental Section

### Materials

Glycerol monomethacrylate (GMA; 99.8%) was donated by GEO Specialty Chemicals (Hythe, UK) and used without further purification. 2-Hydroxypropyl methacrylate (HPMA) was purchased from Alfa Aesar and used as received. Glycidyl methacrylate (GlyMA), 4,4'-azobis(4-cyanopentanoic acid) (ACVA; V-501; 99%), ethanol (99%, anhydrous grade), rhodamine B, thionyl chloride, piperazine, sodium chloride, sodium sulfate, diethyl ether, isopropanol, methanol and dichloromethane were purchased from Sigma-Aldrich UK and were used as received. All solvents were of HPLC quality and were purchased from Fisher Scientific (Loughborough, UK). 4-Cyano-4-(2-phenylethanesulfanylthiocarbonyl)sulfanyl pentanoic acid (PETTC) was prepared and purified as reported elsewhere.<sup>2</sup>

### Preparation of rhodamine B piperazine

#### *Preparation of rhodamine B acid chloride*

Rhodamine B (7.50 g, 16 mmol) was placed in a 50 mL single-neck round-bottomed flask under nitrogen and dissolved in thionyl chloride (7.50 mL, 12.3 g, 103 mmol). After stirring for 22 h, the thionyl chloride was removed via distillation at 100°C. Once complete, the distillation head was removed and the solid was maintained under a flow of nitrogen overnight to remove residual thionyl chloride. The resulting solid was used without further purification; it was stored in the reaction flask and kept in the dark prior to use.

#### *Reaction of rhodamine B acid chloride with piperazine*

Piperazine (5.50 g, 64 mmol) was dissolved in dichloromethane (250 mL). When dissolved, rhodamine B acid chloride (4.00 g, 8.0 mmol) was added dropwise. The reaction mixture was stirred for 21 h, then the solvent was removed at 50°C under reduced pressure and diethyl ether (250 mL) was added, which caused precipitation. The resulting solid was isolated by filtration, dissolved in water (200 mL) and acidified using conc. HCl. The aqueous phase was saturated with sodium chloride and extracted with a 1:2 dichloromethane/isopropanol mixture until colourless (five 100 mL portions). The combined organic fractions were dried over anhydrous sodium sulfate, filtered, and evaporated under vacuum. Finally, the crude rhodamine B piperazine was recrystallized in acetonitrile, filtered and dried under vacuum to give a purple solid. This reagent was used without further purification. TOF MS ES<sup>+</sup>  $m/z$  = 511 (MH<sup>+</sup>); <sup>1</sup>H NMR (400 MHz, CD<sub>2</sub>Cl<sub>2</sub>):  $\delta$  (ppm) = 0.5-1.6 (CH<sub>2</sub>-CH<sub>3</sub>, 12H), 2.0-3.3 (N-CH<sub>2</sub>-CH<sub>2</sub>-N, 7H), 3.3-4.2 (N-CH<sub>2</sub>-CH<sub>3</sub>, 8H), 6.5-8.5 (aromatic, 10 H); <sup>13</sup>C NMR (400 MHz, JMOD, C<sub>2</sub>D<sub>6</sub>OS):  $\delta$  (ppm) = 12 (CH<sub>3</sub>, - polarity), 42-47 (CH<sub>2</sub>, + polarity, 3 signals), 110-170 (aromatic, 13+ signals), 172 (C=O, + polarity). Note that TOF MS and NMR indicated traces of rhodamine B isopropanol impurity.

### Synthesis of poly(glycerol monomethacrylate) (HOOC-PGMA) macro-CTA

GMA (30.0 g, 187 mmol), PETTC (1.156 g, 3.4 mmol; target degree of polymerization = 55), and ACVA (0.191 g, 0.68 mmol; PETTC/ACVA molar ratio = 5.0) were accurately weighed into a 250 mL round-bottomed flask. Anhydrous ethanol (previously purged with nitrogen for 1 h) was then added to produce a 50 % w/w solution, which was placed in an ice bath and purged under nitrogen for 45 min at 0°C. The sealed flask was immersed in an oil bath set at 70°C to initiate the RAFT polymerization of GMA and stirred for 2 h at this temperature. The polymerization was then quenched at approximately 81% conversion by exposure to air, followed by cooling the reaction mixture to room temperature. Methanol (20 mL) was added

to dilute the reaction solution, followed by precipitation into a ten-fold excess of dichloromethane in order to remove unreacted GMA monomer. The precipitate was isolated via filtration and washed with excess dichloromethane before being dissolved in methanol (50 mL). The crude polymer was precipitated for a second time by addition to excess dichloromethane and isolated via filtration. It was then dissolved in water and freeze-dried overnight to afford a yellow solid.  $^1\text{H}$  NMR studies indicated a mean degree of polymerization of 43 via end-group analysis (the integrated aromatic RAFT end-group signals at 7.1-7.4 ppm were compared to those assigned to the two oxymethylene protons at 3.5-4.4 ppm). DMF GPC studies (refractive index detector; calibrated against a series of well-defined poly(methyl methacrylate) (PMMA) standards) indicated an  $M_n$  of  $15,400\text{ g mol}^{-1}$  and an  $M_w/M_n$  of 1.20.

### Synthesis of HOOC-PGMA<sub>43</sub>-*block*-P(HPMA<sub>119</sub>-*co*-GlyMA<sub>1</sub>) diblock copolymer worms via RAFT aqueous dispersion copolymerization of HPMA with GlyMA using HOOC-PGMA<sub>43</sub> macro-CTA

The protocol for the chain extension of HOOC-PGMA<sub>43</sub> macro-CTA via RAFT aqueous dispersion copolymerization of 119 units of HPMA with 1 unit of GlyMA is as follows: PGMA<sub>43</sub> macro-CTA (0.660 g, 0.087 mmol), HPMA monomer (1.500 g, 9.40 mmol), GlyMA monomer (0.012 g, 0.087 mmol), ACVA (8.20 mg, 0.026 mmol; PGMA<sub>43</sub> macro-CTA/ACVA molar ratio = 3.0) were added to a 50 mL round-bottomed flask, prior to addition of water to produce a 10 % w/w solution. The reaction solution was purged under nitrogen for 30 min at 20°C prior to immersion into an oil bath set at 70°C. The reaction mixture was stirred for 4 h at this temperature to ensure almost complete conversion of the HPMA monomer (> 99 % by  $^1\text{H}$  NMR analysis) and was quenched by exposure to air, followed by cooling to ambient temperature. The resulting copolymer worm gel was used without further purification and characterized by DLS, TEM and rheology.

### Reaction of HOOC-PGMA<sub>43</sub>-*block*-P(HPMA<sub>119</sub>-*co*-GlyMA<sub>1</sub>) with rhodamine B piperazine

A typical protocol for the preparation of rhodamine B piperazine-labelled HOOC-*block*-PGMA<sub>43</sub>-P(HPMA<sub>119</sub>-*co*-GlyMA<sub>1</sub>) is as follows: 5.00 g of a 10 % w/w HOOC-PGMA<sub>43</sub>-*block*-P(HPMA<sub>119</sub>-*co*-GlyMA<sub>1</sub>) worm gel (0.50 g copolymer, 20  $\mu\text{mol}$  GlyMA) was weighed into a 20 mL vial equipped with a magnetic stirrer bar and its pH was adjusted from 3.5 to approximately pH 8.0 using sodium hydroxide to produce a worm-to-sphere transition, which in turn induces degelation. Rhodamine B piperazine (2.7 mg, 4.9  $\mu\text{mol}$ ; dye/epoxy molar ratio = 0.25) was accurately weighed out and added to the aqueous dispersion of spherical nanoparticles to give a dye label concentration of  $1.0\text{ mol m}^{-3}$  (or  $1.0\text{ mmol dm}^{-3}$ ). The reaction mixture was stirred overnight at 20°C. After 20 h, the fluorescently-labelled worm gel was dialysed against water for one week (with daily changes of dialysate) so as to remove any unreacted dye. HPLC analysis indicated that 95% of the

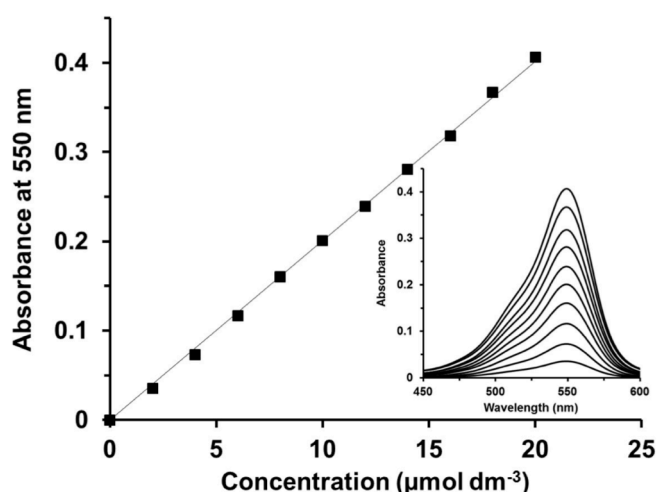


**Figure S1.** Beer-Lambert calibration curve for rhodamine B piperazine in methanol ( $\epsilon = 20,100\text{ dm}^3\text{ mol}^{-1}\text{ cm}^{-1}$ ) obtained using visible absorption spectroscopy at a  $\lambda_{\text{max}}$  of 550 nm

rhodamine B label was covalently grafted to the copolymer worms.

### *Visible absorption spectroscopy*

Spectra were recorded with a PC-controlled UV-1800 Shimadzu spectrophotometer using a 1.0 cm quartz cuvette. A Beer-Lambert linear calibration curve was constructed for the free rhodamine B piperazine dye in methanol with dye concentrations ranging from 2 to 20  $\mu\text{mol dm}^{-3}$ . The maximum absorption was observed at a wavelength of 550 nm and this analysis yielded a molar absorption coefficient of 20,100  $\text{dm}^3 \text{mol}^{-1} \text{cm}^{-1}$ , a factor of  $\sim 5$  less than that for standard rhodamine B.<sup>3</sup> The fraction of HOOC-PGMA<sub>43</sub>-P(HPMA<sub>119</sub>-co-GlyMA<sub>1</sub>) diblock copolymer chains fluorescently labelled with rhodamine B piperazine was determined as follows. Freeze-dried dye-labelled HOOC-PGMA<sub>43</sub>-*block*-P(HPMA<sub>119</sub>-co-GlyMA<sub>1</sub>) diblock copolymer (with a target dye label concentration of 1.0  $\text{mmol dm}^{-3}$ ) was dissolved in methanol to give a 10% w/v copolymer solution. This stock solution was diluted by a factor of 100 using methanol and its absorbance at 550 nm was determined. Using the above molar absorption coefficient for rhodamine B piperazine, the dye concentration was calculated to be 7.2  $\mu\text{mol dm}^{-3}$  (and hence 0.72  $\text{mmol dm}^{-3}$  for the 10% w/v copolymer stock solution). This equates to 3.60  $\mu\text{mol}$  of rhodamine B piperazine in 5.0 mL of 10% w/w HOOC-PGMA<sub>43</sub>-*block*-P(HPMA<sub>119</sub>-co-GlyMA<sub>1</sub>) diblock copolymer worm gel. Comparison of the number of moles of GlyMA (one unit per chain, or 20  $\mu\text{mol}$ ) with that of the rhodamine B piperazine indicates that 18% of diblock copolymer chains are fluorescently labelled (20% chains were targeted). Furthermore, the concentration of rhodamine B piperazine used for the FCS studies is calculated to be 7.2  $\text{nmol dm}^{-3}$ .

### **Preparation of binary mixtures of rhodamine-labelled and unlabelled HOOC-PGMA<sub>43</sub>-P(HPMA<sub>119</sub>-co-GlyMA<sub>1</sub>) worm gels**

The 10% w/w rhodamine B piperazine-labelled HOOC-PGMA<sub>43</sub>-*block*-P(HPMA<sub>119</sub>-co-GlyMA<sub>1</sub>) worm gel (containing a dye label concentration of 1  $\text{mmol dm}^{-3}$ ) was diluted by a factor of one thousand using unlabelled 10% w/w HOOC-PGMA<sub>43</sub>-*block*-P(HPMA<sub>119</sub>-co-GlyMA<sub>1</sub>) copolymer precursor to yield a copolymer worm gel with a final dye label concentration of 1.0  $\text{mmol m}^{-3}$  (or 1.0  $\mu\text{mol dm}^{-3}$ ). This worm gel was diluted further using the unlabelled copolymer worm precursor to afford a final 10% w/w HOOC-PGMA<sub>43</sub>-*block*-P(HPMA<sub>119</sub>-co-GlyMA<sub>1</sub>) worm gel containing a dye label concentration of 10  $\mu\text{mol m}^{-3}$  (or 10  $\text{nmol dm}^{-3}$ ), which was used to study thermo-responsive (de)gelation behaviour by fluorescence correlation spectroscopy (FCS). In the case of pH studies, this latter worm gel was freeze-dried, then redispersed in cold (4°C) aqueous solutions of the desired solution pH to afford various 10% w/w aqueous copolymer dispersions on warming to 20°C. Previous work<sup>4</sup> indicated that these reconstituted gels should possess the same physical properties of the original gels prior to freeze-drying.<sup>4</sup>

## **Instrumentation**

**Fluorescence Correlation Spectroscopy (FCS).** All data were acquired with an inverted LSM510 Meta confocal microscope with an attached ConFocor2 FCS module. The set-up was calibrated through the use of free Rhodamine B (RhB) dye, such that the pinhole dimensions, placement and the filters were optimized. Measurement of the diffusion time for RhB allowed for the calibration of the observation area.

A Linkam FTIR600 stage with a T20 system controller was used to control temperature during FCS measurements when required. The sample (at the same 10% concentration as used for the self-assembly of the worms or spheres) was placed in a Ibidi  $\mu\text{-Dish}^{35\text{mm}}$ , High imaging dish. The temperature was cycled from room temperature down to the desired

temperature for observation. The system was allowed to rest at this temperature for 5 min, the measurement was taken and the system was then returned to room temperature. For studies of the pH dependence, 400  $\mu\text{L}$  of each solution was placed in a separate well of a Nunc Lab-Tek II 8 chamber slide.

Once the sample is placed in the appropriate carrier, a 100  $\mu\text{L}$  droplet of milliQ water was placed upon the objective lens and the carrier was mounted into the microscope with the standard microscope mounting. The objective was raised so that the focal volume could pass through the bottom of the carrier and into the bulk solution. Diffusion measurements were made in this position so that no interfaces were in the focal volume of the microscope.

Each measurement was made for 6 s and repeated 150 times, with any measurements with count rates of less than 1 kHz being discarded.

The LSM-FCS program provided by Carl Zeiss outputs the autocorrelation data as a plain text file. The data within this file were analysed using the software pro Fit (version 6.2, QuantumSoft). The data were then fitted to the autocorrelation function (equation 1 in the article) using the Levenberg-Marquardt algorithm. The diffusion time can then be used in conjunction with the focal volume dimensions to obtain the diffusion coefficient.

**NMR spectroscopy.**  $^1\text{H}$  NMR spectra were recorded using a 400 MHz Bruker  $\mu$  (64 scans were averaged per spectrum).  $^{13}\text{C}$  NMR spectra were recorded using the same instrument (512 scans per spectrum).

**Gel Permeation Chromatography (GPC).** Polymer molecular weights and polydispersities were determined using a DMF GPC set-up operating at  $60^\circ\text{C}$  that comprised two Polymer Laboratories PL gel 5  $\mu\text{m}$  Mixed-C columns connected in series to a Varian 390-LC multi-detector suite (refractive index detector) and a Varian 290-LC pump injection module. The GPC eluent was HPLC-grade DMF containing 10 mM LiBr at a flow rate of  $1.0\text{ mL min}^{-1}$ . DMSO was used as a flow rate marker. Calibration was conducted using a series of ten well defined PMMA standards ( $M_n = 625$  to  $2,480,000\text{ g mol}^{-1}$ ). Chromatograms were analysed using Varian Cirrus GPC software (version 3.3).

**High Performance Liquid Chromatography (HPLC).** Chromatograms (Figure S2) were acquired using a Shimadzu HPLC system consisting of an autosampler (Shimadzu SIL-20AXR), degasser (Shimadzu DGU-20A3), a solvent delivery module (Shimadzu CBM-20A), a diode array detector (Shimadzu SPD-M20A) and a  $150 \times 3.0\text{ mm}$  Jones chromatography Genesis C18  $4\text{ }\mu\text{m}$  column. Samples were prepared as approximately 0.5% solutions in methanol and 10  $\mu\text{L}$  aliquots were injected. Conditions for measurements are as follows: initial eluent = 95:5% v/v water/methanol mixture (initial aqueous phase containing 0.1% trifluoroacetic acid); final eluent = 100%

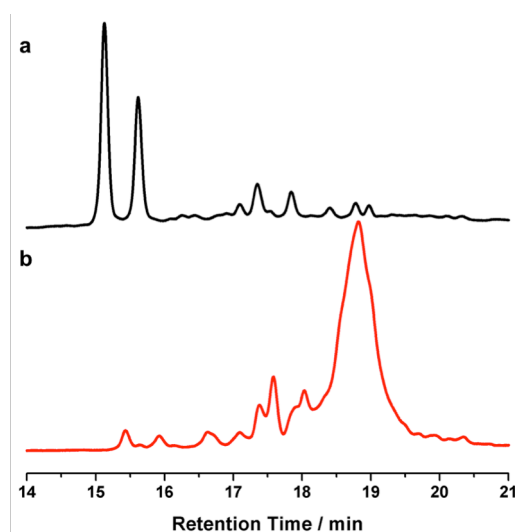


**Figure S2.** Chromatographs obtained by HPLC analysis (UV-visible detector operating at a wavelength of 560 nm) using a gradient eluent (initially 95:5% v/v water/methanol mixture and finally pure methanol; initial aqueous phase contained 0.1% trifluoroacetic acid) for: (a) rhodamine B piperazine dye precursor; (b) rhodamine B-labelled HOOC-PGMA<sub>43</sub>-block-P(HPMA<sub>119</sub>-co-GlyMA<sub>1</sub>) worm gel. This analytical protocol indicated that more than 95% of the dye label was covalently grafted to the copolymer worm gel.

methanol over 20 min, followed by equilibration for 10 min at the original initial eluent composition prior to injection of further samples. Absorbance was determined at a wavelength of 560 nm, which corresponds to the absorption maximum of the dye label.

**Rheology Studies.** Storage ( $G'$ ) and loss ( $G''$ ) moduli of the HOOC-PGMA<sub>43</sub>-P(HPMA<sub>119</sub>-co-GlyMA<sub>1</sub>) worm gel were measured as a function of percentage strain, angular frequency and temperature using an AR-G2 rheometer equipped with a variable temperature Peltier plate and a 40 mm 2° aluminium cone to assess critical gelation temperatures and gel strengths. Temperature sweeps were conducted using an angular frequency of 1.0 rad s<sup>-1</sup> and a strain of 1.0 %. In this experiment (Figure S3), the  $G'$  and  $G''$  values were measured between 25°C and 4°C at 1.0°C intervals, allowing an equilibration time of two minutes between each measurement.

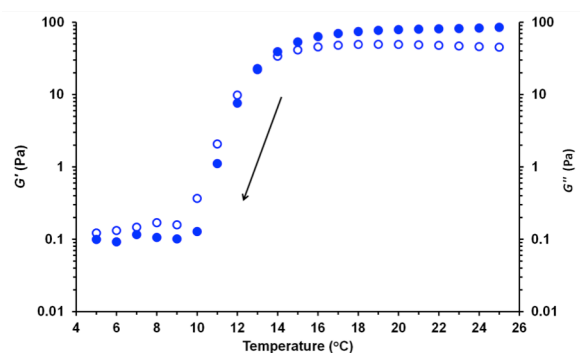


**Figure S3.** Temperature dependence of the storage modulus ( $G'$  – closed circles) and loss modulus ( $G''$  – open circles) for a 10 % w/w aqueous dispersion of HOOC-PGMA<sub>43</sub>-*block*-P(HPMA<sub>119</sub>-co-GlyMA<sub>1</sub>). The cross-over of the two curves indicates the critical gelation temperature, which is estimated to be 13°C. Conditions: angular frequency = 1.0 rad s<sup>-1</sup> at an applied strain of 1.0%.

**Transmission Electron Microscopy (TEM).** Polymer solutions were diluted 100-fold at 20°C to generate 0.10% w/w dispersions. Images obtained at lower pH were prepared by diluting solutions in acidic water. Copper/palladium TEM grids (Agar Scientific) were coated in-house to yield a thin film of amorphous carbon. The grids were then subjected to a plasma glow-discharge for 30 s to create a hydrophilic surface. Individual samples (0.10% w/w, 12 μL) were adsorbed onto the grids for one minute and then blotted with filter paper to remove excess solution. A uranyl formate (0.75% w/w) solution (9 μL) was soaked on the sample-loaded grid for 20 s to stain the polymer. This was then blotted to remove excess uranyl formate solution. The grids were dried using a vacuum hose. Imaging was performed on a Phillips CM100 instrument at 100 kV, equipped with a Gatan 1 k CCD camera.

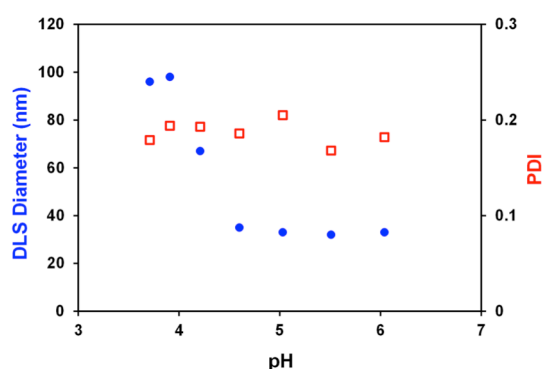


**Figure S4.** pH dependence of the hydrodynamic diameter (and DLS dispersity, PDI) for a 0.10 % w/w aqueous dispersion of HOOC-PGMA<sub>43</sub>-*block*-P(HPMA<sub>119</sub>-co-GlyMA<sub>1</sub>) recorded at 25°C using a Malvern Nanosizer ZS instrument. The particle size at around pH 5-6 corresponds to spheres, whereas that observed just below pH 4 corresponds to the sphere-equivalent diameter for worms with PDI ≈ 0.25. The dramatic size reduction between pH 4.0 and 4.6 corresponds to the worm-to-sphere transition, as previously reported.<sup>1</sup>

**Dynamic Light Scattering (DLS).** DLS studies were conducted using a Malvern Zetasizer NanoZS instrument at 25°C. Studies were performed on 0.10% w/w aqueous dispersions in disposable cuvettes at a fixed scattering angle of 173° (Figure S4). Intensity-average hydrodynamic diameters were calculated via the Stokes-Einstein equation using a non-negative least-squares (NNLS) algorithm. All data were averaged over three consecutive runs.

## References

1. J. R. Lovett, N. J. Warren, L. P. D. Ratcliffe, M. K. Kocik and S. P. Armes, *Angew. Chem. Int. Ed.*, 2015, **54**, 1279-1283.
2. E. R. Jones, M. Semsarilar, A. Blanz and S. P. Armes, *Macromolecules*, 2012, **45**, 5091-5098.
3. L. F. Mottram, S. Forbes, B. D. Ackley and B. R. Peterson, *Beilstein J. Org. Chem.*, 2012, **8**, 2156-2165.
4. M. K. Kocik, O. O. Mykhaylyk and S. P. Armes, *Soft Matter*, 2014, **10**, 3984-3992.

## Data

The data contained in the manuscript are tabulated below. FCS autocorrelation data include data outside of the region plotted in the inset to Figure 3. Since the data below are taken directly from the files used in the generation of the figures, the number of significant figures, particularly in the uncertainty columns, is greater than would be required for an accurate representation of the results.

### Diffusion coefficients

Figure 3

Temperature (K)	Diffusion coefficient, $D$ ( $\text{m}^2 \text{s}^{-1}$ )	$\Delta D$ ( $\text{m}^2 \text{s}^{-1}$ )
278	$2.03 \times 10^{-11}$	$9.40 \times 10^{-12}$
281	$1.60 \times 10^{-11}$	$6.78 \times 10^{-12}$
284	$1.49 \times 10^{-11}$	$2.02 \times 10^{-12}$
285	$1.04 \times 10^{-11}$	$1.95 \times 10^{-12}$
287	$3.28 \times 10^{-12}$	$8.28 \times 10^{-13}$
288	$3.57 \times 10^{-12}$	$6.56 \times 10^{-13}$
292	$3.64 \times 10^{-12}$	$1.51 \times 10^{-13}$
295	$3.64 \times 10^{-12}$	$4.06 \times 10^{-13}$
298	$3.57 \times 10^{-12}$	$6.49 \times 10^{-13}$

Figure 4

pH	Diffusion coefficient, $D$ ( $\text{m}^2 \text{s}^{-1}$ )	$\Delta D$ ( $\text{m}^2 \text{s}^{-1}$ )
3.02	$2.86 \times 10^{-12}$	$9.15 \times 10^{-14}$
3.53	$3.13 \times 10^{-12}$	$1.29 \times 10^{-13}$
3.93	$2.67 \times 10^{-12}$	$2.30 \times 10^{-13}$
4.47	$2.21 \times 10^{-11}$	$3.22 \times 10^{-12}$
4.89	$2.00 \times 10^{-11}$	$1.07 \times 10^{-12}$
5.41	$2.13 \times 10^{-11}$	$9.18 \times 10^{-13}$
6.1	$2.15 \times 10^{-11}$	$6.01 \times 10^{-13}$



## FCS data

$\tau$ (s)	G( $\tau$ ) [T = 284 K]	G( $\tau$ ) [T = 288 K]
$2.00 \times 10^{-7}$	12.31883	17.78858
$4.00 \times 10^{-7}$	3.09381	3.34859
$6.00 \times 10^{-7}$	2.2267	2.89017
$8.00 \times 10^{-7}$	2.24174	2.60545
$1.00 \times 10^{-6}$	2.12288	2.01773
$1.20 \times 10^{-6}$	2.45165	1.86427
$1.40 \times 10^{-6}$	2.10685	1.98777
$1.60 \times 10^{-6}$	2.01742	2.01227
$1.80 \times 10^{-6}$	2.01954	2.3681
$2.00 \times 10^{-6}$	2.12892	1.97458
$2.20 \times 10^{-6}$	1.84258	2.21544
$2.40 \times 10^{-6}$	1.84228	1.99671
$2.60 \times 10^{-6}$	1.85366	1.8627
$2.80 \times 10^{-6}$	2.0506	2.01406
$3.00 \times 10^{-6}$	1.99384	2.08299
$3.20 \times 10^{-6}$	2.01739	1.79809
$3.60 \times 10^{-6}$	2.03377	1.97856
$4.00 \times 10^{-6}$	2.17423	1.80924
$4.40 \times 10^{-6}$	1.8934	2.14206
$4.80 \times 10^{-6}$	1.96037	2.13404
$5.20 \times 10^{-6}$	2.08601	1.74621
$5.60 \times 10^{-6}$	2.08127	1.76771
$6.00 \times 10^{-6}$	1.84526	2.31194
$6.40 \times 10^{-6}$	1.97402	1.87915
$7.20 \times 10^{-6}$	1.93692	2.08455
$8.00 \times 10^{-6}$	1.79044	2.00659
$8.80 \times 10^{-6}$	1.93859	1.86466
$9.60 \times 10^{-6}$	1.9922	2.01564
$1.04 \times 10^{-5}$	1.93719	1.9989
$1.12 \times 10^{-5}$	1.92633	2.08958
$1.20 \times 10^{-5}$	1.99891	1.892
$1.28 \times 10^{-5}$	2.00277	2.11599
$1.44 \times 10^{-5}$	1.96567	1.98275
$1.60 \times 10^{-5}$	1.85585	2.00313
$1.76 \times 10^{-5}$	1.95912	1.92274
$1.92 \times 10^{-5}$	1.92367	2.02451
$2.08 \times 10^{-5}$	1.85675	1.97422

$2.24 \times 10^{-5}$	1.91766	1.9955
$2.40 \times 10^{-5}$	1.89644	1.95009
$2.56 \times 10^{-5}$	1.7965	2.01388
$2.88 \times 10^{-5}$	1.86082	1.91127
$3.20 \times 10^{-5}$	1.86287	1.94004
$3.52 \times 10^{-5}$	1.81613	1.91946
$3.84 \times 10^{-5}$	1.8224	1.97239
$4.16 \times 10^{-5}$	1.79122	1.97304
$4.48 \times 10^{-5}$	1.75307	1.92952
$4.80 \times 10^{-5}$	1.80209	1.93334
$5.12 \times 10^{-5}$	1.76017	1.95735
$5.76 \times 10^{-5}$	1.7699	1.94242
$6.40 \times 10^{-5}$	1.73151	1.92454
$7.04 \times 10^{-5}$	1.71201	1.94683
$7.68 \times 10^{-5}$	1.67751	1.88293
$8.32 \times 10^{-5}$	1.67574	1.85118
$8.96 \times 10^{-5}$	1.66495	1.90932
$9.60 \times 10^{-5}$	1.68338	1.93022
$1.02 \times 10^{-4}$	1.66622	1.88986
$1.15 \times 10^{-4}$	1.64122	1.84967
$1.28 \times 10^{-4}$	1.62146	1.84866
$1.41 \times 10^{-4}$	1.588	1.84725
$1.54 \times 10^{-4}$	1.56981	1.81768
$1.66 \times 10^{-4}$	1.53974	1.82943
$1.79 \times 10^{-4}$	1.5439	1.79567
$1.92 \times 10^{-4}$	1.51199	1.80855
$2.05 \times 10^{-4}$	1.52566	1.80088
$2.30 \times 10^{-4}$	1.48226	1.74585
$2.56 \times 10^{-4}$	1.48201	1.74881
$2.82 \times 10^{-4}$	1.44868	1.75362
$3.07 \times 10^{-4}$	1.42741	1.70337
$3.33 \times 10^{-4}$	1.39822	1.68632
$3.58 \times 10^{-4}$	1.38826	1.69523
$3.84 \times 10^{-4}$	1.38397	1.66957
$4.10 \times 10^{-4}$	1.37671	1.66059
$4.61 \times 10^{-4}$	1.33453	1.64989
$5.12 \times 10^{-4}$	1.31557	1.60817
$5.63 \times 10^{-4}$	1.29806	1.59282
$6.14 \times 10^{-4}$	1.28117	1.59001

$6.66 \times 10^{-4}$	1.28061	1.57103
$7.17 \times 10^{-4}$	1.24739	1.53197
$7.68 \times 10^{-4}$	1.2352	1.52398
$8.19 \times 10^{-4}$	1.23169	1.50898
$9.22 \times 10^{-4}$	1.21685	1.48826
$1.02 \times 10^{-3}$	1.2005	1.47035
$1.13 \times 10^{-3}$	1.19137	1.4516
$1.23 \times 10^{-3}$	1.16977	1.43453
$1.33 \times 10^{-3}$	1.16423	1.42872
$1.43 \times 10^{-3}$	1.14641	1.40155
$1.54 \times 10^{-3}$	1.14072	1.36688
$1.64 \times 10^{-3}$	1.13563	1.3632
$1.84 \times 10^{-3}$	1.1154	1.34142
$2.05 \times 10^{-3}$	1.10638	1.31138
$2.25 \times 10^{-3}$	1.09461	1.30297
$2.46 \times 10^{-3}$	1.09351	1.28681
$2.66 \times 10^{-3}$	1.08265	1.26911
$2.87 \times 10^{-3}$	1.07728	1.26053
$3.07 \times 10^{-3}$	1.06998	1.24732
$3.28 \times 10^{-3}$	1.06753	1.23166
$3.69 \times 10^{-3}$	1.06122	1.21246
$4.10 \times 10^{-3}$	1.05366	1.19122
$4.51 \times 10^{-3}$	1.04857	1.18392
$4.92 \times 10^{-3}$	1.04772	1.16617
$5.32 \times 10^{-3}$	1.04134	1.15169
$5.73 \times 10^{-3}$	1.03915	1.1497
$6.14 \times 10^{-3}$	1.03741	1.13947
$6.55 \times 10^{-3}$	1.03161	1.12865
$7.37 \times 10^{-3}$	1.03171	1.11537
$8.19 \times 10^{-3}$	1.02416	1.10368
$9.01 \times 10^{-3}$	1.02502	1.09109
$9.83 \times 10^{-3}$	1.02186	1.08349
0.01065	1.01968	1.07709
0.01147	1.0217	1.07378
0.01229	1.01864	1.06631
0.01311	1.01822	1.06159
0.01475	1.01396	1.05697
0.01638	1.01329	1.04872
0.01802	1.01528	1.04612

0.01966	1.01282	1.03793
0.0213	1.01083	1.03683
0.02294	1.00993	1.03622
0.02458	1.0121	1.03137
0.02621	1.00828	1.03158
0.02949	1.00904	1.02719
0.03277	1.00968	1.02242
0.03604	1.00834	1.02173
0.03932	1.00709	1.02138
0.0426	1.0078	1.01627
0.04588	1.00749	1.01385
0.04915	1.00757	1.01548
0.05243	1.00692	1.01218
0.05898	1.00679	1.01313
0.06554	1.00715	1.01114
0.07209	1.00477	1.01009
0.07864	1.00539	1.00954
0.0852	1.00468	1.00853
0.09175	1.0054	1.00739
0.0983	1.00531	1.00803
0.10486	1.00578	1.00657
0.11796	1.00492	1.00659
0.13107	1.00449	1.006
0.14418	1.00498	1.00491
0.15729	1.00468	1.00547
0.17039	1.00402	1.00283
0.1835	1.00376	1.00417
0.19661	1.00379	1.0046
0.20972	1.00415	1.0034
0.23593	1.00385	1.00407
0.26214	1.00338	1.00377
0.28836	1.00366	1.00394
0.31457	1.00352	1.00343
0.34079	1.00358	1.00343
0.367	1.00309	1.00418
0.39322	1.00322	1.00371
0.41943	1.00313	1.00316
0.47186	1.00281	1.00282
0.52429	1.00281	1.00282

0.57672	1.0025	1.00323
0.62915	1.0028	1.00216
0.68157	1.00234	1.00288
0.734	1.00281	1.003
0.78643	1.00234	1.00245
0.83886	1.00249	1.00273
0.94372	1.00292	1.00228
1.04858	1.00271	1.00262
1.15343	1.00284	1.00232
1.25829	1.00275	1.00216
1.36315	1.00274	1.00251
1.46801	1.00257	1.00209
1.57286	1.0025	1.00192
1.67772	1.00265	1.00222
1.88744	1.00209	1.00296
2.09715	1.00227	1.00298
2.30687	1.00223	1.00323
2.51658	1.00222	1.00296
2.7263	1.00229	1.00276
2.93601	1.0022	1.00262
3.14573	1.00212	1.00257
3.35544	1.00213	1.00275
3.77487	1.00149	1.00188
4.1943	1.00123	1.00177
4.61373	1.001	1.00206
5.03316	1.00095	1.00239
5.4526	1.00118	1.00229
5.87203	1.00134	1.00222
6.29146	1.00106	1.00265
6.71089	1.00127	1.00262
7.54975	1.00092	1.00336
8.38861	1.00084	1.00352
9.22747	1.00053	1.00358
10.06633	1.00084	1.00362
10.90519	1.0007	1.00299
11.74405	1.0011	1.00253
12.58291	1.00087	1.00256
13.42177	1.00054	1.00252
15.09949	1.00166	1.00322

16.77722	1.0015	1.00206
18.45494	1.00142	1.00217
20.13266	1.00057	1.00253
21.81038	1.00028	1.00406
23.4881	1.00011	1.00385
25.16582	0.99952	1.00328
26.84355	0.99888	1.00326